Environ. Sci. Technol. **2000**, *34,* 3159−3166

Influence of Reduction Reactions and Solid-Phase Composition on Porewater Concentrations of Arsenic

H. MCCREADIE* AND D. W. BLOWES
Department of Earth Sciences, University of Waterloo, Waterloo, Ontario, Canada, N2L 3G1

C. J. PTACEK
Environment Canada, National Water Research Institute, Burlington, Ontario, Canada, L7R 4A6

J. L. JAMBOR
Leslie Investments, 316 Rosehill Wynd, Tsawwassen, British Columbia, Canada, V4M 3L9

An increasing amount of attention is being focused on the effects of arsenic on health and the factors that control arsenic mobility in groundwater. The release and transport of arsenic below the water table in the current tailings impoundment at Campbell Mine in Balmertown, ON, Canada, are controlled by the reduction of ferric oxide phases within the saturated tailings. The activity of chemolithotrophic bacteria is indicated by enriched $\delta^{34}S-SO_4$ ratios, high alkalinity, depleted $\delta^{13}C-CO_3$ ratios, and low SO_4 concentrations, all of which are consistent with bacterially mediated Fe and SO_4 reduction. The concentrations of Fe and As in the tailings porewater increase with depth. This increase is attributed to the bacterially mediated reduction of As-rich hematite and maghemite. The maximum concentrations of Fe and As are 20 and 100 mg/L, respectively. At the bottom of the impoundment, As concentrations decrease sharply to 0.3 mg/L. This decrease in concentration is attributed to reprecipitation of the As as a diagenetic As-bearing sulfide phase.

Introduction

Arsenic has been documented in groundwater at concentrations of 0.08−48 mg/L, up to 3 orders of magnitude greater than the U.S. EPA drinking water limit of 0.050 mg/L (*1, 2*). Some of these elevated concentrations are associated with nickel, cobalt, and gold mines. Many sulfide ore bodies contain arsenopyrite and other arsenical sulfides that are disposed with the mill tailings either as waste products or as unrecovered ore minerals. Because the tailings porewater from many tailings impoundments enters the subjacent groundwater system and because arsenic is mobile in many groundwater environments, the potential transport of arsenic from tailings impoundments into groundwater systems is an environmental concern.

Arsenic-bearing solids may occur as reduced phases or as oxidized phases. Reduced phases, such as arsenical sulfides, are susceptible to oxidative dissolution when exposed to oxygen. Several studies, including an investigation at the Campbell Mine gold-tailings impoundment in Balmertown, ON, Canada, have demonstrated the importance of this mechanism (*3−5*).

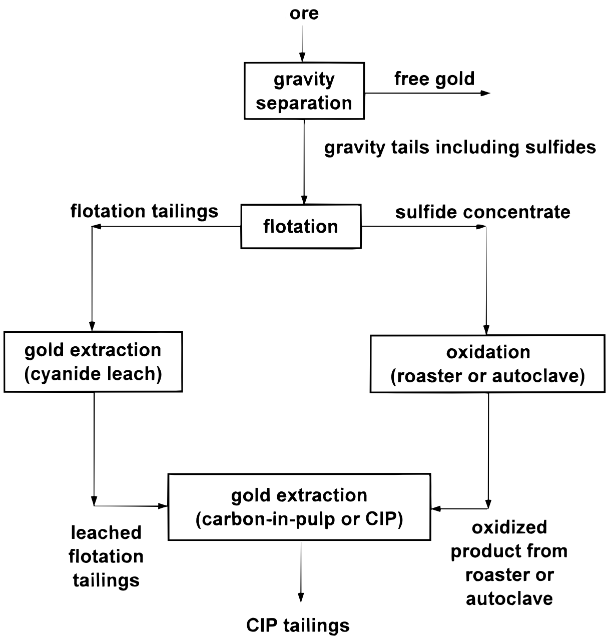

FIGURE 1. Simplified flow sheet for a mill process with an oxidation circuit. This circuit oxidizes a sulfide concentrate, which is then leached. The residue is discharged to the tailings impoundment together with waste (gangue) sulfides from the flotation circuit.

In contrast to reduced phases such as arsenopyrite, oxidized phases are potentially susceptible to dissolution in the saturated zone. Oxidized phases occur in tailings as a result of oxidation of sulfide concentrates during processing (Figure 1). The nature of the oxidized phase is partly controlled by the type of concentrate feed and the process used to oxidize it. A common process involves roasting concentrate at high temperature to oxidize and drive off sulfur. At the Campbell Mine gold-tailings impoundment in Balmertown, ON, Canada, these oxidized residues contain hematite [α-Fe_2O_3] and maghemite [γ-Fe_2O_3] with associated arsenic. These residues were deposited on organic-rich sediments, which produce conditions that are conducive to the growth and activity of facultative, heterotrophic bacteria. These bacteria can reduce Fe(III) in oxidized iron phases, including hematite (*6−8*). This study characterizes the porewater and solid-phase profiles from the Campbell Mine tailings and demonstrates the influence of solid-phase composition and reducing reactions on arsenic concentrations.

Site Description

The Campbell Mine gold-tailings impoundment is in Balmertown, ON, about 250 km northeast of Winnipeg, MB (Figure 2). The climate is humid continental, with average annual total precipitation of 595 mm. Average monthly temperatures range from −21 to 18 °C.

Hydrogeologic Setting. The bedrock in the area of Campbell Mine forms an irregular surface with a relief of more than 20 m over distances of a few hundred meters. Isolated, knob-shaped bedrock outcrops have resulted from the infilling of bedrock valleys by glacial and interglacial deposits. These deposits include glacial till, outwash and

---

* Corresponding author present address: Waterloo Hydrogeologic, 180 Columbia Street West−Unit 1104, Waterloo, Ontario, Canada, N2L 3L3; telephone: (519)746-1798; fax: (519)885-5262; e-mail: hmccreadie@flowpath.com.

10.1021/es991194p CCC: $19.00

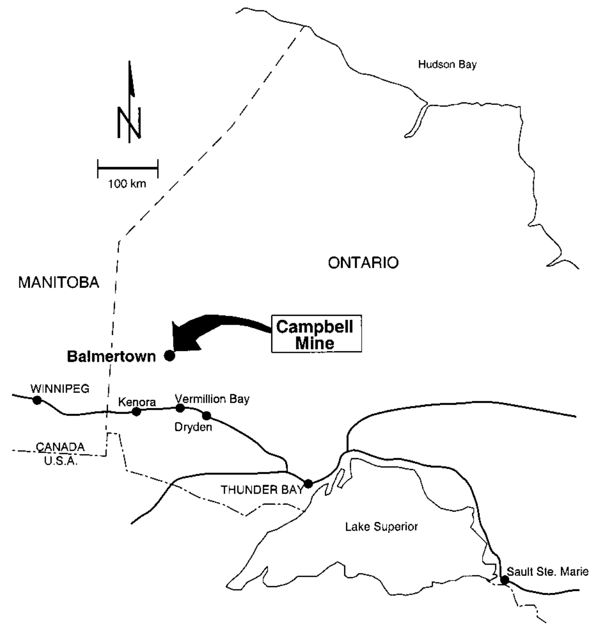

FIGURE 2. Location of Campbell Mine.

subwash sands and gravels, and overlying glacial-lake clays. Consistent with the regional stratigraphy, the sequence in proximity to the Campbell tailings areas consists of bedrock, silty till, sandy till, sand, silty clay, and peat.

Tailings Deposition. Tailings have been deposited in several areas near the mine, including the Detta Lake area, the 7th Street area, the Balmer area, and the Current Impoundment. This paper focuses on the tailings in the Current Impoundment, which is bounded by three water-retaining dams (Figure 3). These tailings cover an area of 60 ha and are up to 4 m thick.

Milling. The ore at Campbell Mine is split into two streams with a froth–flotation circuit. Both streams from this circuit are leached with cyanide to extract the gold. However, prior to cyanide leaching in a carbon-in-pulp (CIP) circuit, the sulfide concentrate is oxidized (Figure 1). The ore was originally oxidized in a roaster (1951–1991) and is currently oxidized in an autoclave (1991–present). Each of these streams has a distinct mineralogical assemblage that has a direct impact on the evolution of the porewater chemistry in the tailings impoundment.

Methodology

Tailings Solids. Samples of tailings solids were collected at 14 locations in 5-cm-diameter, thin-walled aluminum tubing using the Starr and Ingleton (*9*) technique. The cores were split in half, wrapped in plastic, and frozen in the field. The cores were transported to the laboratory frozen. Selected samples were examined using a variety of mineralogical methods. Thin sections were examined microscopically in both reflected and transmitted light. X-ray diffraction patterns were obtained using a Rigaku rotating-anode diffractometer and Cu X-radiation. As well, numerous patterns were obtained using the Debye–Scherrer method and Co X-radiation. Qualitative microbeam analyses and X-ray maps for specific elements were obtained with a JEOL 820 scanning electron microscope; a JEOL 733 electron microprobe at CANMET, Natural Resources Canada, was used to obtain quantitative analyses. Selected samples of the tailings and peat were analyzed for ^{13}C. The total sulfur content of 86 tailings samples was analyzed using a Leco induction furnace.

Porewater. Porewater samples were extracted from the saturated zone by squeezing tailings cores by a method similar to that described by Blowes and Jambor (*10*). Each sample was filtered through a 0.45-μm, cellulose–nitrate filter. Measurements of pH and E_h were made in the field using an Orion combination pH electrode (model 815600) and an Orion platinum redox electrode (model 96-7800BN). The pH electrode was calibrated in pH 4 and pH 7 buffers and checked at regular intervals. The E_h electrode was checked in ZoBell's solution (*11*) and Light's solution (*12*), also at regular intervals. Alkalinity titrations were performed in the field with methyl red, bromcresol green indicator, and sulfuric acid using a Hach Chemical Company digital titrator. Two samples were collected from each core section: one was acidified with 12 N, analytical-grade HCl for cation analysis and the other was left unacidified for anion analysis. The concentrations of Al, Sb, As, Ba, Be, Bi, B, Cd, Ca, Cr, Co, Cu, Fe, Pb, Li, Mg, Mn, Mo, Ni, P, K, Se, Si, Ag, Na, Sr, Tl, Sn, Ti, W, V, and Zn were analyzed by inductively coupled plasma atomic emission spectrophotometry (ICP-AES). Samples with low As concentrations were also analyzed by atomic absorption spectroscopy (AAS) after hydride generation. Chloride and SO_4 were analyzed by ion chromatography (IC). Selected unacidified samples were analyzed for NO_3 by IC, and selected acidified samples were analyzed for NH_4 by colorimetry. Selected samples were analyzed for dissolved organic carbon (DOC) by catalytic oxidation followed by infrared detection.

Porewater samples from the saturated zone were also collected from PVC piezometers. The piezometers were pumped dry the day before sampling. Measurements of pH and E_h were made in a sealed flow-through cell that was maintained at porewater temperature. Alkalinity was measured in the field by the same method as the squeezed samples. Aqueous sulfide concentrations were determined in the field using the colorimetric method of Lindsay and Baedecker (*13*). Samples from the piezometers were collected with a peristaltic pump and polyethylene tubing and were filtered through a 0.45-μm, in-line, cellulose–nitrate filter. Samples were acidified in the same manner as the squeezed samples. Selected samples were speciated into As(III) and As(V) in the field by the anion exchange method of Ficklin (*14*) and were analyzed by AAS after hydride generation or by ICP-AES. Selected samples were also collected and analyzed for $^{34}S-SO_4$ and $^{13}C-CO_3$ in the Environmental Isotope Laboratory at the University of Waterloo.

Data Interpretation. The porewater data were interpreted with the aid of the equilibrium geochemical model MINTEQA2 (*15*). The thermodynamic database of MINTEQA2 was modified to be consistent with that of WATEQ4F (*16*).

Results and Discussion

The CIP tailings in the Current Impoundment are derived from two separate streams within the mill: the tailings from the flotation circuit and the oxidized residue from the oxidation circuit. Each of these streams has a distinct mineralogical composition.

Flotation Tailings. The flotation tailings consist mainly of dolomite and quartz, reflecting the hydrothermal genesis of the ore body, and occur throughout the full depth of the tailings impoundment (Figure 3). The average composition of the dolomite ($n = 24$) is $Ca_{0.980}Mg_{0.759}Fe_{0.247}Mn_{0.014}(CO_3)_2$. Minor quantities of calcite and ferroan magnesite were also detected. Chlorite [$(Mg,Fe^{2+})_5Al(Si_3Al)O_{10}(OH)_8$] is the third most abundant mineral. Other silicates, namely, muscovite [$KAl_2(AlSi_3)O_{10}(OH)_2$], talc [$Mg_3Si_4O_{10}(OH)_2$], amphibole [$Ca_2(Mg,Fe)_5Si_8O_{22}(OH)_2$], and albite [$NaAlSi_3O_8$], occur in smaller quantities.

Small quantities of sulfides (total sulfur 0.5 wt % as S or 1.4 wt % as FeS) occur in the flotation tailings. Pyrrhotite [$Fe_{1-x}S$] is the most abundant sulfide mineral. Most of the pyrrhotite is liberated but some occurs as inclusions in

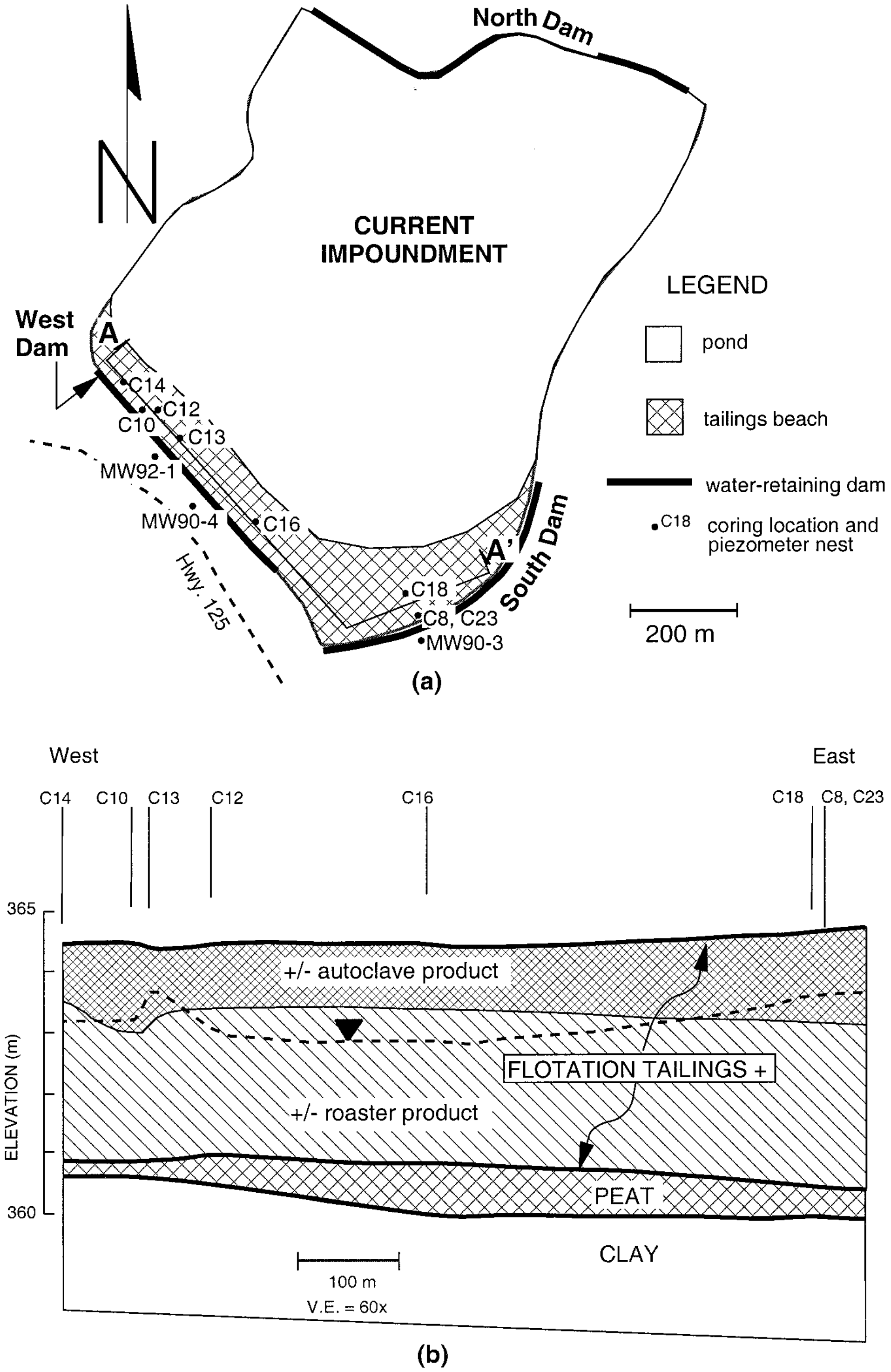

FIGURE 3. (a) Core and piezometer locations in the Current Impoundment. (b) Tailings stratigraphy in the Current Impoundment, section A−A′.

silicates. The next most abundant sulfides are arsenopyrite [FeAsS] and sphalerite [(Zn,Fe)S], with much smaller quantities of pyrite [FeS_2] and traces of chalcopyrite [$CuFeS_2$]. Arsenopyrite [FeAsS] is the main source of arsenic in the flotation tailings and occurs mostly as inclusions in silicates. Gersdorffite [NiAsS] is also present but only in trace quantities. Because it is an active deposition area, the sulfides in the Current Impoundment have not yet oxidized, except for occasional paleo-oxidation seams.

Oxidized Residue from the Autoclave. The oxidized residue from the autoclave occurs in the upper 1.5 m of the tailings impoundment. The mineralogical character of the autoclave product is distinct from the roaster but does not have a bearing on the geochemical reactions discussed in this paper. The geochemistry of this product is described in detail by McCreadie et al. (*17*).

Oxidized Residue from the Roaster. The oxidized residue from the roaster occurs in the lower 2.6 m (Figure 3) as traces throughout and as discrete layers. The lower meter of tailings contains abundant quantities and shallower depths contain less. The As-rich phases in this residue are hematite [α-Fe_2O_3] and maghemite [γ-Fe_2O_3]. These phases occur as porous

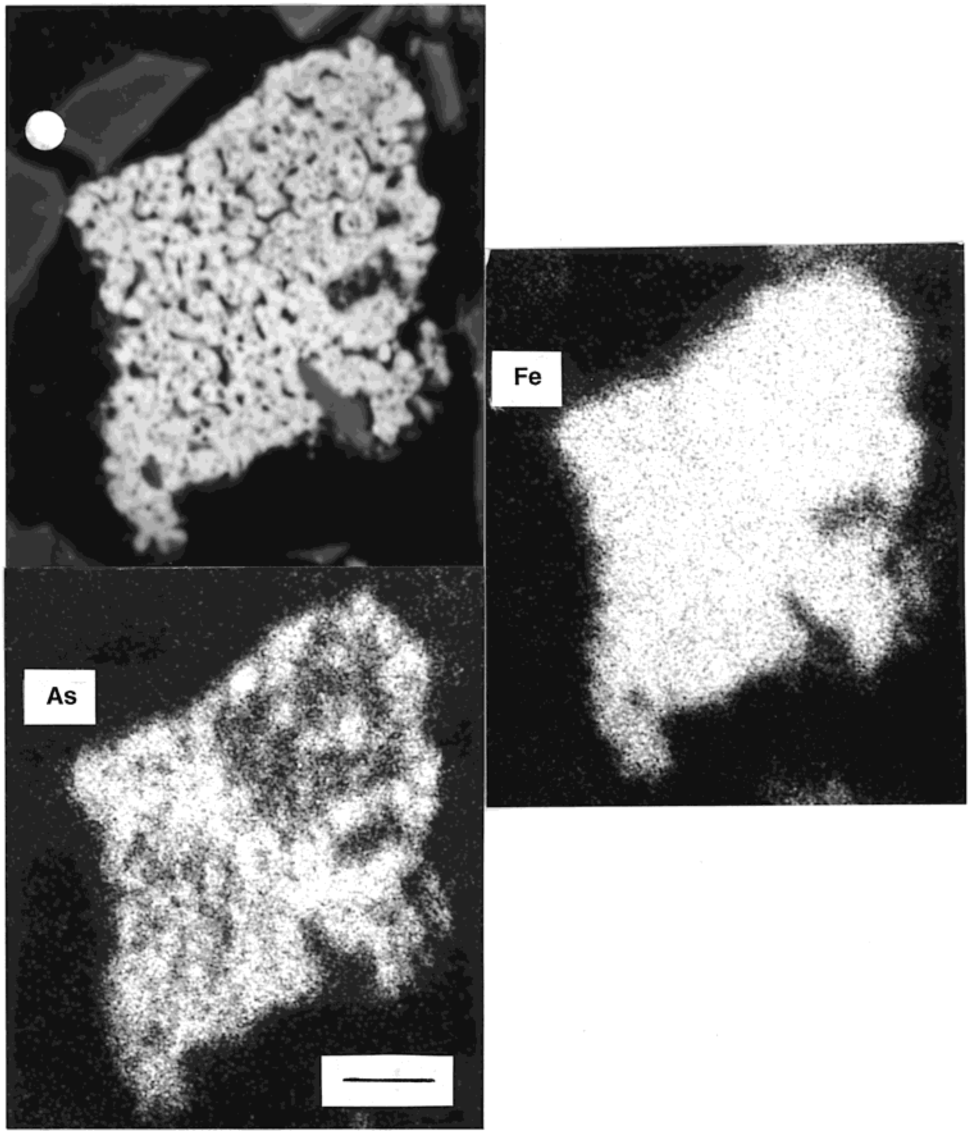

FIGURE 4. Back-scattered electron image of porous iron oxide from the roaster. X-ray maps show that iron is evenly distributed throughout the grain but arsenic is unevenly distributed. The arsenic may be adsorbed. Bar scale represents 10 μm.

grains (Figure 4) with typical sizes of 20−50 μm. These grains have inclusions of a variety of gangue minerals and also have a high As content (Figure 4), which varies widely between and within grains but is not correlated with the type of iron oxide. The As was presumably incorporated during the roasting process. No discrete As phases were identified on the surfaces of the grains, and the As is not part of the crystal structure.

Flow Regime within Current Impoundment. The hydraulic head in the sand aquifer under the Current Impoundment is consistently below the pond and water table elevation in the impoundment. The downward gradient across the clay in the area of South Dam during the summer of 1995 was about 0.3. Consistently downward gradients have also been measured within the tailings impoundment (*5*). No seepage has been observed on the face of the dam, indicating downward flow into the underlying sand aquifer.

Process Water Parameters. Process water is the water that is discharged from the mill to the tailings impoundment. The process water within the tailings shows two distinct compositions, reflecting the change from the roaster to the autoclave in 1991. The autoclave process water seems to be confined to the upper 3.5 m of the tailings and is characterized by higher concentrations of Ca, Mg, Na, K, and SO_4 (Figure 5). The water below 3.5 m is derived from the process water that was discharged prior to commissioning the autoclave. A 1.6-m downward displacement of this concentration front between 1991 and 1994 is consistent with the downward flow direction that has been inferred from the piezometric measurements (*5*). The trends in porewater composition below 3.5 m, including the porewater within the peat, are attributed to diagenetic reactions because the measured and calculated rate of downward movement indicates that the original porewater has already moved through the zone where these samples were collected.

Sulfate Reduction. Sulfur isotope analyses show that $^{34}S-SO_4$ is enriched in the bottom meter at C23 (Figure 5). This sulfate reduction reaction is a diagenetic reaction that seems to be altering the original porewater composition. The ambient $\delta^{34}S-SO_4$ ratio is about 6‰ and increases in the bottom meter to 40‰ (Figure 5), which is indicative of sulfate reduction (*18*). Other locations show similar trends (*5*). Sulfate reduction can be written as follows:

$$SO_4^{2-} + 2CH_2O \rightarrow 2HCO_3^- + HS^- + H^+ \qquad (1)$$

The available data are all consistent with the sulfate reduction reaction. Dissolved organic carbon occurs in the

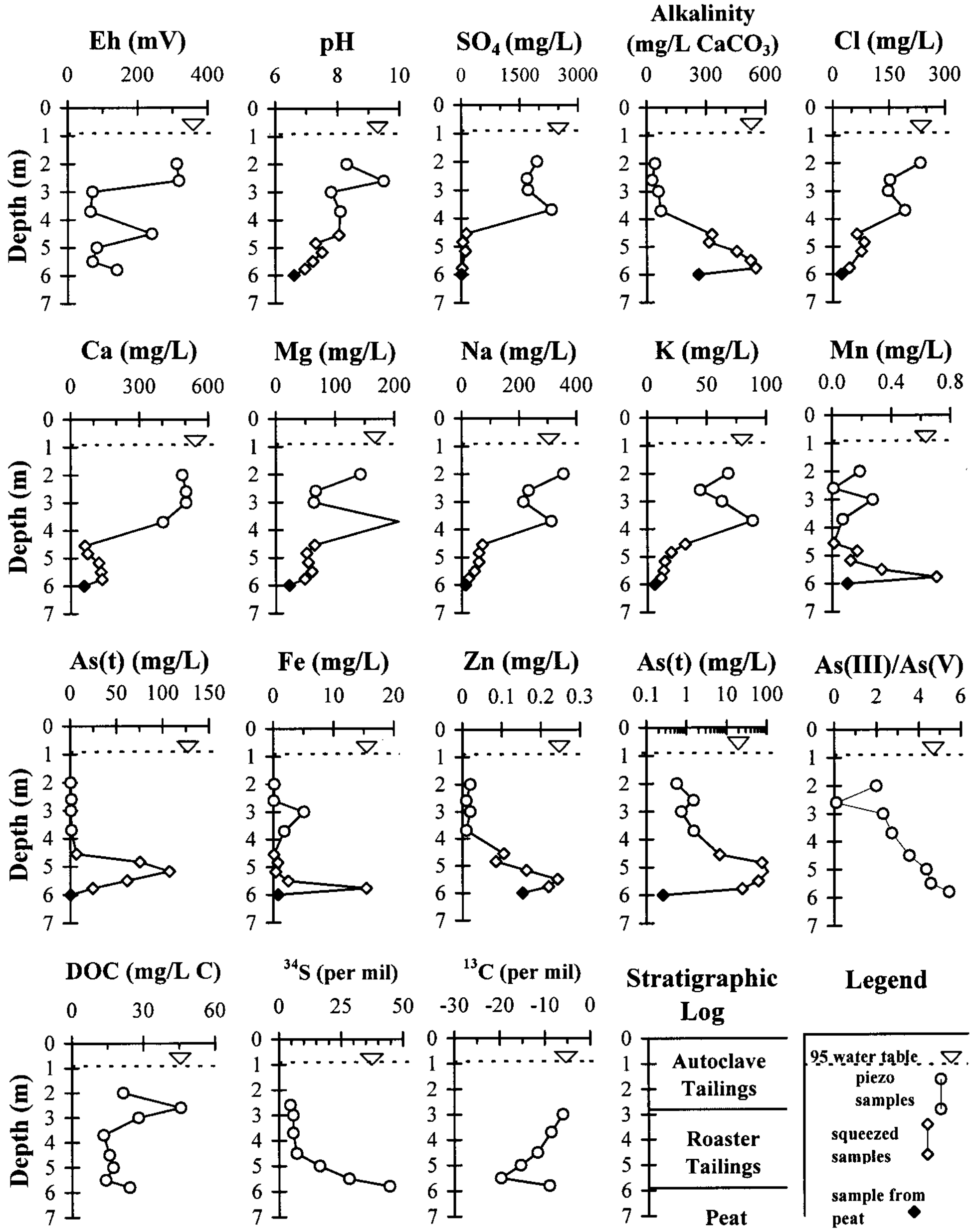

FIGURE 5. Water chemistry profiles for location C23. Samples are from piezometers for 2.0−3.7 m depth and from squeezing for 4.55−6.0 m depth, except for E_h, DOC, δ^{34}S−SO$_4$, and δ^{13}C−CO$_3$, which are from piezometers. The filled symbol at the bottom of the profile indicates a porewater sample from the peat. The second profile of As(t) is shown on a log scale to illustrate the arsenic concentrations at shallow depth.

porewater at concentrations that range from 16 to 24 mg/L in this zone, indicating that an organic carbon source is available for this reaction. Sulfate decreases from 2300 mg/L at 3.7 m depth to 22 mg/L at 5.8 m; alkalinity increases from 72 to 550 mg/L; and pH decreases from 8.1 to 6.6 (Figure 5). All of these trends are consistent with SO$_4$ reduction and are observed consistently throughout the Current Impoundment (Figure 6) and at the south end of the Balmer area (*5*). Although the decrease in SO$_4$ concentrations with depth may be partly attributable to dilution from recharge of urban runoff at C23, the change in isotopic signature indicates that much of the decrease is attributable to SO$_4$ reduction. In other areas of the impoundment, SO$_4$ concentrations decrease with depth even though concentrations of Cl do not (*5*). The decrease in SO$_4$ concentrations causes the water to become undersaturated with respect to gypsum below 3.7 m depth at C23 (Table 1).

Measured δ^{13}C−CO$_3$ ratios at C23 decrease from a maximum of −6 ‰ at a depth of 3.0 m to a minimum of −20‰ at a depth of 5.5 m (Figure 5). The organic carbon in the peat has a δ^{13}C ratio of −27‰ whereas the average (n = 2) δ^{13}C ratio of the carbonates in the tailings is +0.4‰. The depleted δ^{13}C−CO$_3$ ratios within the reducing zone indicate that the dissolved inorganic carbon (DIC) is a mixture of process water-derived and peat-derived sources and that the peat-derived DIC becomes more prevalent with depth. The inverse relationships between δ^{13}C−CO$_3$ ratios and δ^{34}S−SO$_4$ ratios, and between δ^{13}C−CO$_3$ ratios and alkalinity at a depth from 3.0 to 5.5 m suggest that the organic carbon in the peat is a source of DIC in the porewater as a result of SO$_4$ reduction. Depleted δ^{13}C−CO$_3$ ratios probably result from bacterial oxidation of the peat and are consistent with the observed changes in SO$_4$ concentrations. Murphy and Davis (*19*) and Chapelle et al. (*20*) have made similar interpretations of δ^{13}C−CO$_3$ ratios in the Milk River aquifer, AB, Canada, and in the Black Creek aquifer, South Carolina, respectively. The E_h values in the sulfate-reducing zone range from approximately 50 to 150 mV (Figure 5), which is higher than

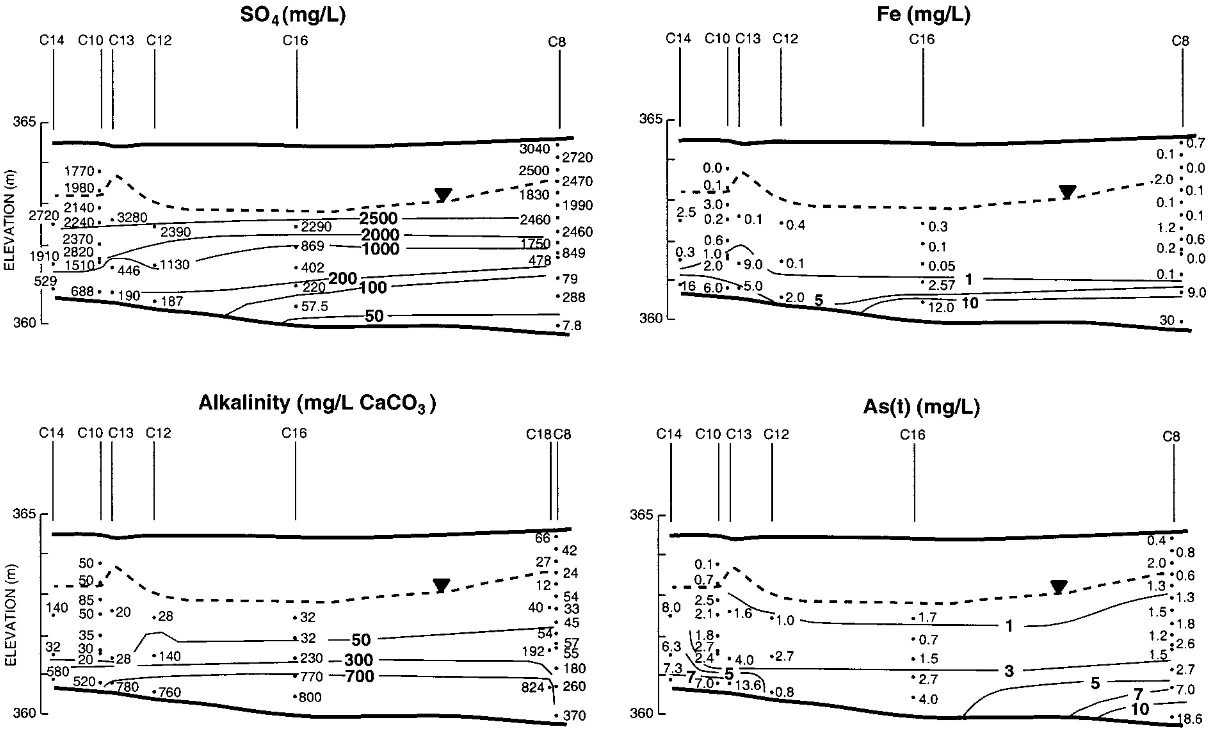

FIGURE 6. Contours of SO_4, alkalinity, Fe, and As in the Current Impoundment, section A−A′, 1994.

TABLE 1. Saturation Indices for Selected Minerals at Selected Depths

nest	depth (m)	calcite	dolomite	magnesite	gypsum	siderite (d)	$AlAsO_4$	$Ca_3(AsO_4)_2$	$Cu_3(AsO_4)$	$FeAsO_4$	$Mn_3(AsO_4)_2$	ferrihydrite	hematite	maghemite
C23	2.0	0.515	0.552	−0.456	−0.062	−3.967	−6.534	−6.012	−9.775	−5.221	−6.911	3.429	19.024	10.256
	3.0	0.238	−0.364	−1.095	−0.050	−0.112	−4.920	−6.685	−8.658	−5.800	−7.077	1.735	15.636	6.868
	3.7	0.452	0.671	−0.273	−0.099	−0.250	−5.528	−5.930	−10.024	−5.810	−7.825	2.030	16.225	7.457
	4.5	0.149	0.349	−0.293	−0.751	−3.166	−6.460	−6.675	−10.558	−5.406	−9.628	3.089	18.343	9.575
	5.0	0.601	1.301	0.207	−1.683	−0.393	−4.825	−6.351	−8.377	−5.697	−9.140	1.481	15.127	6.359
C23S	5.5	0.286	0.242	−0.536	n.a.	0.040	−1.188	−4.963	−4.667	−3.240	−3.882	1.137	14.438	5.670
	5.8	0.067	−0.303	−0.862	−2.112	0.610	−1.000	−6.358	−5.489	−3.153	−4.278	1.187	14.538	5.770
	6.0	−0.886	−2.172	−1.779	−2.761	−1.210	−2.380	−12.145	−8.992	−6.762	−11.251	−1.035	10.094	1.325

would be expected from sulfate-reducing or iron-reducing reactions. This result suggests that an analysis of specific dissolved constituents is sometimes required to determine the geochemical processes that are occurring rather than relying on E_h measurements.

The cause of the increase in $\delta^{13}C-CO_3$ at a depth of 5.8 m is unclear but may be partly due to methanogenesis by reduction of CO_2 because methanogenic bacteria preferentially reduce $^{12}C-CO_2$ (*19*).

Arsenic Release Zone. The As release zone occurs near the bottom of the tailings impoundment within the zone of SO_4 reduction. At C23, As concentrations are consistently between 0.5 and 1.5 mg/L from 2.0 to 4.5 m depth. At a depth of 5.2 m, the As increases to a maximum concentration of 107 mg/L (Figure 5). This pattern is repeated in five of seven profiles throughout the Current Impoundment (Figure 6), in the profile in the Balmer area that overlies peat (*5*), and in a profile in the nearby Detta Lake tailings area (unpublished data). The majority of As occurs as As(III) at C23 (Figure 5) and in all other profiles (*5*).

Anomalously high concentrations of dissolved Fe also occur within the arsenic release zone. At C23, dissolved Fe concentrations are consistently between 0.1 and 1.8 mg/L to a depth of 5.0 m but increase to a maximum of 15 mg/L at a depth of 5.8 m (Figure 5). This pattern is observed in all profiles throughout the Current Impoundment (Figure 6) and in the Balmer area profile that overlies peat (*5*). (Iron was not determined for the Detta Lake profile.)

One possible source of Fe and As is the oxidation of arsenical sulfides that are contained within the tailings. However, mineralogical analysis of three tailings cores revealed only minor paleo-oxidation rims on some of the sulfide grains, indicating that the sulfides are not significantly oxidized within the Current Impoundment tailings. These sulfide minerals, therefore, are not the source of Fe and As observed in the porewater.

The most likely source of the high concentrations of dissolved Fe and As in the reducing zone is dissolution of porous texture hematite and maghemite in the roaster tailings. Reductive dissolution is inferred because these minerals are relatively insoluble. Laboratory experiments with hematite indicate that dissolution rates are orders of magnitude greater in the presence of a reductant (*21*). Biotic reduction of ferric oxides has been demonstrated in laboratory studies with pure cultures of bacteria (*6*), in laboratory studies with bacterial cultures from anoxic lake sediments (*8*), and in a field study of groundwater systems (*7*). The enriched $\delta^{34}S-SO_4$ ratios in the bottom meter of the Campbell tailings suggest that sulfate-reducing bacteria are active in this zone. Reduction of the roaster-derived ferric oxides can be described by

$$2Fe_2O_3{\cdot}xH_3AsO_3 + CH_2O + 7H^+ \Rightarrow 4Fe^{2+} + HCO_3^- + 4H_2O + 2xH_3AsO_3 \quad (2)$$

where *x* is the amount of (nonstructural) As associated with the hematite grains in the roaster tailings.

Moore et al. (*22*) and Moncure et al. (*23*) hypothesized a similar reaction to explain As release in the reducing zone of the Milltown Reservoir sediments, and Postma (*24*) suggested that a similar reaction occurs in swamp sediments. Notably, this reaction seems to be occurring even though the equilibrium calculations indicate that the porewater is supersaturated with respect to the iron oxide phases hematite and maghemite (Table 1).

Some of the Fe that is released by reaction 2 remains in solution rather than precipitating as an Fe−S phase. The inverse relationship between dissolved SO_4 and Fe concentrations suggests that the supply of dissolved sulfide from SO_4 reduction is insufficient to precipitate all of the Fe as a sulfide phase.

The occurrence of abundant hematite and maghemite within the SO_4-reducing zone indicates that SO_4 is being reduced before all of the solid-phase Fe(III) has been consumed, suggesting kinetic limitations on the reduction of crystalline iron oxides relative to dissolved SO_4. Lovley and Phillips (*25*) suggested similar limitations in developing a rapid assay technique for measuring the amount of microbially reducible Fe in sediments.

The increase in dissolved As from 6.6 mg/L at a depth of 4.6 m to 100 mg/L at a depth of 5.2 m (Figure 5) probably indicates that the top of the reducing zone occurs at 4.6 m. This depth is consistent with the shape of the $^{34}S-SO_4$ profile, which shows enrichment of $^{34}S-SO_4$ starting at 4.6 m depth (Figure 5). Equilibrium geochemical modeling indicates that the porewater is undersaturated with respect to all of the arsenate phases in the WATEQ4F database (Table 1), suggesting that the depth trends in dissolved As concentrations are not controlled by equilibrium reactions involving any of those phases.

Arsenic Precipitation Zone. In contrast with dissolved Fe, Si, Mn, Ni, and Zn, which have maximum concentrations at a depth of 5.8 m (Figure 5), dissolved As decreases abruptly from a maximum concentration of 100 mg/L at 5.2 m to 0.3 mg/L at 6.0 m (Figure 5). The lower dissolved As concentrations below 5.2 m suggest that the dissolved As is being removed from solution, possibly as an As sulfide. Dissolved sulfide was not detectable at a detection limit of 0.015 mg/L, suggesting that any sulfide released by sulfate reduction is consumed in a secondary precipitation reaction. The diagenetic precipitation of As may be in minerals such as orpiment (As_2S_3), realgar (AsS), arsenopyrite (FeAsS), or as a less crystalline precursor precipitate.

Precipitation of these phases or poorly crystalline precursors has been postulated in similar geochemical environments. For example, Moore et al. (*22*) used selective extraction techniques to determine whether sulfide precipitation is immobilizing some of the As in the reducing zone of the Milltown Reservoir sediments. Moncure et al. (*23*) agreed with the hypothesis of Moore et al. (*22*). Similarly, Postma (*24*) observed diagenetic pyrite in brackish and freshwater swamp sediments, and many researchers have observed diagenetic iron sulfides in ocean sediments (e.g., ref *25*).

pH Buffering. The pH of the porewater ranges from 9.5 to 6.6 and generally decreases with depth (Figure 5). The abundant quantities of ferroan dolomite within the tailings will probably maintain the porewater at near-neutral values for an extended period of time. Equilibrium geochemical modeling results indicate that the porewater is generally supersaturated with respect to calcite and dolomite from a depth of 2.0−5.0 m in the samples from the piezometers and from a 4.6−5.5 m depth in the samples from the core (Table 1). The sample at 5.8 m is near saturation with respect to calcite and is undersaturated with respect to dolomite. The sample at 6.0 m, which was collected from the peat at the impoundment base, is undersaturated with respect to dolomite and calcite. These results indicate that dolomite and calcite are thermodynamically stable in the shallow tailings.

Implications for Tailings Management

The results of this investigation have implications for tailings management practices, all of which are being observed at the Campbell Mine. For example, adding organic carbon to tailings should be avoided in cases where the impoundment contains autoclave or roaster residues. The results of this investigation suggest that addition of organic carbon to tailings may stimulate reducing bacteria, which tend to destabilize these oxidized phases. Adding organic carbon to impoundments that contain weathered sulfides in the unsaturated zone may also result in reductive dissolution, i.e., a reversal of the oxidation process that initially immobilized the metals in the unsaturated zone (*26*). Organic carbon is sometimes added to tailings surfaces in the form of sewage sludge, a practice that is being investigated to alleviate the problem of sludge disposal and encourage revegetation within abandoned tailings impoundments.

Similarly, flooding the tailings on closure is more likely to destabilize any oxidized phases. Flooding the tailings will limit the amount of oxygen that can penetrate the tailings, a condition that is more likely to promote the development of reducing conditions. The availability of oxygen tends to limit the reduction of oxidized phases because of the preferential reduction of oxygen.

Disposal of oxidized tailings on top of peat may have no net effect on As loading from tailings impoundments as long as the flow direction is downward, sufficient quantities of labile organic C are available to nourish the bacteria, adequate SO_4 is available to reprecipitate the As as an iron−arsenic sulfide, and the residence time is sufficient to allow the reaction to proceed to completion. These findings indicate that a mass balance analysis, and an assessment of geochemical reaction rates and groundwater velocity are required to determine the environmental implications of tailings disposal.

Acknowledgments

Financial support for this research was provided by Placer Dome North America, Campbell Mine, and the Natural Sciences and Engineering Research Council of Canada. Klohn-Crippen Consultants provided financial support to H.M. during the research. The authors gratefully acknowledge the dedicated field support of Mike Moncur and Tim Adams.

Literature Cited

(1) Welch, A. H.; Lico, M. S.; Hughes, J. L. *Ground Water* **1988**, *26*, 333−344.

(2) Davis, A.; Kempton, J. H.; Nicholson, A. *Appl. Geochem.* **1994**, *9*, 569−582.

(3) Smyth, D. J. A. Hydrogeological and Geochemical Studies Above the Water Table in an Inactive Uranium Tailings Impoundment Near Elliot Lake, Ontario. M.Sc. Project, University of Waterloo, Waterloo, Ontario, 1981.

(4) Blowes, D. W. The Geochemistry, Hydrogeology and Mineralogy of Decommissioned Sulfide Tailings: A Comparative Study. Ph.D. Thesis, University of Waterloo, Waterloo, Ontario, 1990.

(5) McCreadie, H. Release and Transport of Arsenic in a Gold-Mine Tailings Impoundment. M.Sc. Thesis, University of Waterloo, Waterloo, Ontario, 1996.

(6) Arnold, R. G.; DiChristina, T. J.; Hoffmann, M. R. *Biotechnol. Bioeng.* **1988**, *32*, 1081−1096.

(7) Lovley, D. R.; Baedecker, M. J.; Lonergan, D. J.; Cozzarelli, I. M.; Phillips, E. J. P.; Siegel, D. I. *Nature* **1989**, *339*, 297−299.

(8) Lovley, D. R.; Phillips, E. J. P.; Lonergan, D. J. *Environ. Sci. Technol.* **1991**, *25*, 1062−1067.

(9) Starr, R. C.; Ingleton, R. A. *Ground Water Monit. Rev.* **1992**, *41*, 91−95.

(10) Blowes, D. W.; Jambor, J. L. *Appl. Geochem.* **1990**, *5*, 327−346.

(11) Nordstrom, D. K. *Geochim. Cosmochim. Acta* **1977**, *41*, 1835−1841.
(12) Light, T. S. *Anal. Chem.* **1972**, *44*, 1038−1039.
(13) Lindsay, S. S.; Baedecker, M. J. *Ground Water Contamination: Field Methods, ASTM STP 963*; Collins, A. G., Johnson, A. I., Eds.; American Society for Testing and Materials: Philadelphia, 1986; pp 349−357.
(14) Ficklin, W. H. *Talanta* **1983**, *30*, 371−373.
(15) Allison, J. D.; Brown, D. S.; Novo-Gradac, K. J. *MINTEQA2/PRODEFA2. A geochemical assessment model for environmental systems: version 3.0 user's manual*; Environmental Research Laboratory, U.S. Environmental Protection Agency: Washington, DC, 1990; 106 pp.
(16) Ball, J. W.; Nordstrom, D. K. *User's manual for WATEQ4F, with revised thermodynamic data base and test cases for calculating speciation of major, trace and redox elements in natural water*; U.S. Geological Survey Open File Report 91-183; USGS: Denver, 1991.
(17) McCreadie, H.; Jambor, J. L.; Blowes, D. W.; Ptacek, C.; Hiller, D. Geochemical Behavior of Autoclave-Produced Ferric Arsenates and Jarosite in a Gold-Mine Tailings Impoundment. In *Waste Characterization and Treatment*; Proceedings from Annual Meeting and Exhibit, March 9−11, 1998, Waste Characterization and Treatment Symposium; Petruk, W., Ed.; Society for Mining, Metallurgy and Exploration Inc.: 1998; pp 61−78.
(18) Jones, G. E.; Starkey, R. L. *Appl. Microbiol.* **1957**, *5*, 111−118.
(19) Murphy, E. M.; Davis, S. N. *Water Resour. Res.* **1989**, *25*, 1893−1905.
(20) Chapelle, F. H.; Morris, J. T.; McMahon, P. B.; Zelibor, J. L. *Geology* **1988**, *16*, 117−121.
(21) Appelo, C. A. J.; Postma, D. *Geochemistry, Groundwater and Pollution*; A. A. Balkema: Rotterdam/Brookfield, 1993; pp 281−282.
(22) Moore, J. H.; Ficklin, W. H.; Johns, C. *Environ. Sci. Technol.* **1988**, *22*, 432−437.
(23) Moncure, G. M.; Jankowski, P. A.; Drever, J. I. The hydrochemistry of arsenic in reservoir sediments, Milltown, Montana, USA. *Water-Rock Interaction, Proceedings of the 7th International Symposium on Water-Rock Interaction*, Park City, UT, July 13−18, 1992; Kharaka, Y. K., Maest, A. S., Eds.; WRI-7.
(24) Postma, D. *Am. J. Sci.* **1982**, *282*, 1151−1183.
(25) Lovley, D. R.; Phillips, E. J. P. *Appl. Env. Microbiol.* **1987**, *53*, 1536−1540.
(26) Ribet, I.; Ptacek, C. J.; Blowes, D. W.; Jambor, J. L. *J. Contam. Hydrol.* **1995**, *17*, 239−273.

Received for review October 18, 1999. Revised manuscript received May 1, 2000. Accepted May 1, 2000.

ES991194P